

# Targeting the DP2 receptor alleviates muscle atrophy and diet-induced obesity in mice through oxidative myofiber transition

Huying Ning<sup>1</sup>, Huiwen Ren<sup>1</sup>, Yan Zhao<sup>1</sup>, HaiFang Yin<sup>2</sup>, Zhenji Gan<sup>3</sup>, Yujun Shen<sup>1\*</sup> & Ying Yu<sup>1\*</sup>

<sup>1</sup>Department of Pharmacology, Tianjin Key Laboratory of Inflammatory Biology, Center for Cardiovascular Diseases, Key Laboratory of Immune Microenvironment and Disease (Ministry of Education), The Province and Ministry Co-sponsored Collaborative Innovation Center for Medical Epigenetics, School of Basic Medical Sciences, Tianjin Medical University, Tianjin, China; <sup>2</sup>Department of Cell Biology and Key Laboratory of Immune Microenvironment and Disease (Ministry of Education), Tianjin Medical University, Tianjin, China; <sup>3</sup>State Key Laboratory of Pharmaceutical Biotechnology and MOE Key Laboratory of Model Animals for Disease Study, Department of Spine Surgery, Nanjing Drum Tower Hospital, The Affiliated Hospital of Nanjing University Medical School, Jiangsu Key Laboratory of Molecular Medicine, Chemistry and Biomedicine Innovation Center (ChemBIC), Model Animal Research Center, Nanjing University Medical School, Nanjing University, Nanjing, China

## Abstract

**Background** Mammalian skeletal muscles consist of two main fibre types: slow-twitch (type I, oxidative) and fast-twitch (type IIa, fast oxidative; type IIb/IIx, fast glycolytic). Muscle fibre composition switch is closely associated with chronic diseases such as muscle atrophy, obesity, type II diabetes and athletic performance. Prostaglandin D<sub>2</sub> (PGD<sub>2</sub>) is a bioactive lipid derived from arachidonic acid that aggravates muscle damage and wasting during muscle atrophy. This study aimed to investigate the precise mechanisms underlying PGD<sub>2</sub>-mediated muscle homeostasis and myogenesis.

**Methods** Skeletal muscle-specific PGD<sub>2</sub> receptor DP2-deficient mice (DP2<sup>fl/fl</sup>HSA<sup>Cre</sup>) and their littermate controls (DP2<sup>fl/fl</sup>) were subjected to exhaustive exercise and fed a high-fat diet (HFD). X-linked muscular dystrophy (MDX) mice and HFD-challenged mice were treated with the selective DP2 inhibitor CAY10471. Exercise tolerance, body weight, glycometabolism and skeletal muscle fibre composition were measured to determine the role of the skeletal muscle PGD<sub>2</sub>/DP2 signalling axis in obesity and muscle disorders. Multiple genetic and pharmacological approaches were also used to investigate the intracellular signalling cascades underlying the PGD<sub>2</sub>/DP2-mediated skeletal muscle fibre transition.

**Results** PGD<sub>2</sub> generation and DP2 expression were significantly upregulated in the hindlimb muscles of HFD-fed mice ( $P < 0.05$  or  $P < 0.01$  vs. normal chow diet). Compared with DP2<sup>fl/fl</sup> mice, DP2<sup>fl/fl</sup>HSA<sup>Cre</sup> mice exhibited remarkable glycolytic-to-oxidative fibre-type transition in hindlimb muscles and were fatigue resistant during endurance exercise ( $154.9 \pm 6.0$  vs.  $124.2 \pm 8.1$  min,  $P < 0.05$ ). DP2<sup>fl/fl</sup>HSA<sup>Cre</sup> mice fed an HFD showed less weight gain ( $P < 0.05$ ) and hepatic lipid accumulation ( $P < 0.01$ ), reduced insulin resistance and enhanced energy expenditure ( $P < 0.05$ ) compared with DP2<sup>fl/fl</sup> mice. Mechanistically, DP2 deletion promoted the nuclear translocation of nuclear factor of activated T cells 1 (NFATc1) by suppressing RhoA/Rho-associated kinase 2 (ROCK2) signalling, which led to enhanced oxidative fibre-specific gene transcription in muscle cells. Treatment with CAY10471 enhanced NFATc1 activity in the skeletal muscles and ameliorated HFD-induced obesity ( $P < 0.05$  vs. saline) and insulin resistance in mice. CAY10471 also enhanced exercise tolerance in MDX mice ( $100.8 \pm 8.0$  vs.  $68.9 \pm 11.1$  min,  $P < 0.05$  vs. saline) by increasing the oxidative fibre-type ratio in the muscles ( $45.1 \pm 2.3\%$  vs.  $32.3 \pm 2.6\%$ ,  $P < 0.05$  vs. saline).

**Conclusions** DP2 activation suppresses oxidative fibre transition via RhoA/ROCK2/NFATc1 signalling. The inhibition of DP2 may be a potential therapeutic approach against obesity and muscle disorders.

**Keywords** DP2 receptor; muscle fibre; NFATc1; oxidative; prostaglandin D<sub>2</sub>

Received: 28 June 2022; Revised: 19 October 2022; Accepted: 27 October 2022

\*Correspondence to: Ying Yu, MD, PhD, and Yujun Shen, PhD, Department of Pharmacology, School of Basic Medical Sciences, Tianjin Medical University, 22 Qixiangtai Road, Heping District, Tianjin 300070, China. Email: yuying@tmu.edu.cn and yujun\_shen@tmu.edu.cn  
Huying Ning, Huiwen Ren and Yan Zhao have equal contribution.

## Introduction

In mammals, skeletal muscle comprises approximately 40–55% of the body mass and functions to generate forces and regulate whole-body energy metabolism. Mammalian skeletal muscles are composed of two major types of muscle fibres: slow-twitch (type I, oxidative) and fast-twitch (type II) fibres. The latter can be further divided into fast oxidative (type IIa) and fast glycolytic (type IIb/IIx) fibres. Oxidative fibres are rich in mitochondria and display aerobic metabolism and fatigue resistance. In contrast, glycolytic fibres primarily use anaerobic glycolysis as their ATP source for rapid force, but they fatigue quickly. The components of muscle fibre types mediate their susceptibility or resistance to muscle or metabolic disorders, such as Duchenne muscular dystrophy (DMD), obesity and type 2 diabetes. For instance, DMD sequentially degenerates glycolytic and oxidative fibres, whereas genetic or pharmacological activation of oxidative fibres ameliorates DMD symptoms.<sup>1</sup> Patients with type 2 diabetes have reduced proportions of oxidative fibres,<sup>2</sup> which are positively correlated with whole-body insulin sensitivity.<sup>3</sup> In contrast, an oxidative-to-glycolytic fibre-type switch leads to severe dilated cardiomyopathy in mice.<sup>4</sup> Thus, oxidative skeletal fibres confer molecular, cellular and physiological benefits in muscle and metabolic disorders, and targeting oxidative fibre transition may be a novel therapeutic strategy for these diseases.<sup>1</sup>

Skeletal muscle fibre-type specification begins from embryonic development and shifts after birth via intrinsic genetic and epigenetic programs and extrinsic factors such as neural input and hormonal influence.<sup>5</sup> Several transcription factors, including nuclear factor of activated T cells 1 (NFATc1) and PPAR $\gamma$  coactivator (PGC)-1 $\alpha$ , play central roles in controlling oxidative muscle fibre transition. NFAT acts as a muscle nerve sensor and maintains the oxidative fibre phenotype by promoting oxidative gene expression and suppressing glycolytic gene transcription.<sup>6</sup> PGC-1 $\alpha$  drives mitochondrial biogenesis and protects oxidative fibres from denervation-induced muscle atrophies.<sup>7</sup> These transcription factors convert environmental signals at the cell surface to phenotypic changes in skeletal muscle fibres. Neural impulses, cytokines (transforming growth factor- $\beta$ , tumour necrosis factor- $\alpha$  and myostatin)<sup>8</sup> and hormones (glucocorticoids and thyroid hormone)<sup>9,10</sup> are the main environmental signal components. Recently, metabolites derived from glucose, proteins and lipids have emerged as novel modulators of muscle fibre specification.<sup>11,12</sup> However, the precise role of these metabolites in muscle fibre remodelling remains unclear.

Prostaglandins (PGs), a subgroup of bioactive lipid metabolites, including PGD<sub>2</sub>, PGE<sub>2</sub>, PGF<sub>2 $\omega$</sub> , PGI<sub>2</sub> and thromboxane A<sub>2</sub>, are derived from arachidonic acid through a reaction se-

quentially catalysed by cyclooxygenase (COX)-1/2 and PG synthase. PGs perform essential functions in skeletal muscle homeostasis and plasticity by binding to a family of G protein-coupled receptors in an autocrine- and paracrine-dependent manner.<sup>13</sup> PGs such as PGF<sub>2 $\omega$</sub> , PGE<sub>2</sub> and PGI<sub>2</sub> exhibit pro-myogenic effects by promoting the growth, fusion and survival of myoblasts.<sup>13</sup> In contrast, leukocyte-derived PGD<sub>2</sub> inhibits the onset of myogenesis during the early stages of inflammation<sup>14</sup> and the blockage of haematopoietic prostaglandin D synthase (HPGDS) ameliorates injury-induced muscle necrosis and genetic muscular dystrophy in mice.<sup>15</sup> These results indicate a unique role for PGD<sub>2</sub> signalling in skeletal muscle myogenesis. However, whether PGD<sub>2</sub> and its receptors (DP1 and DP2) regulate myofiber plasticity, thereby affecting the progression of muscular dystrophy and metabolic diseases, remains unknown.

In this study, we found that PGD<sub>2</sub>/DP2 signalling was activated in the skeletal muscles of high-fat diet (HFD)-challenged and X-linked muscular dystrophy (MDX) mice. Muscle-specific deletion of DP2 promoted glycolytic-to-oxidative muscle fibre transition and attenuated HFD-induced obesity and insulin resistance in mice. Furthermore, the nuclear translocation of NFATc1, which controls oxidative fibre gene expression, was significantly increased in DP2-deficient muscle cells. A DP2 agonist inhibited the oxidative fibre-type switch by impeding NFATc1 nuclear entry via Gi/RhoA/Rho-associated kinase 2 (ROCK2)-mediated NFATc1 phosphorylation at Ser243. Treatment with the selective DP2 inhibitor CAY10471 ameliorated HFD-induced obesity in mice and improved muscle atrophy in MDX mice.

## Methods

### Mice

Male mice (6–8 weeks old) with a C57BL/6 background were used for the experiments. Wild-type (WT) mice were purchased from Beijing Vital River Laboratory Animal Technology Company. DP1 global knockout (DP1 KO), DP2 KO, DP2<sup>flox/flox</sup> (DP2<sup>fl/fl</sup>) and MDX mice were maintained in our laboratory.<sup>16,17</sup> DP2<sup>fl/fl</sup> mice were crossed with human skeletal actin Cre (HSA<sup>Cre</sup>) mice<sup>18</sup> to generate DP2<sup>fl/fl</sup>HSA<sup>Cre</sup> mice. Mice were maintained in an environment with a controlled temperature (22  $\pm$  1°C) and relative humidity (50  $\pm$  5%) on a 12:12-h light/dark cycle, with free access to a normal chow diet (ND) and water. All the experiments were conducted using age-matched controls. All animal experiments were performed in accordance with the guidelines and approval of the Institutional Animal Care and Use Committee of the Tianjin Medical University.

### High-fat diet-induced obesity

Mice were fed an ND (MD12031, Mediceance) or an HFD (MD12033, Mediceance) for 12 weeks. Food intake and body weight were monitored weekly. Body composition analysis was performed using Echo MRI (Echo Medical Systems, Houston, TX, USA).

### CAY10471 treatment

Mice were fed an HFD for 12 weeks to induce obesity and were treated with CAY10471 (10 mg/kg, i.p., every other day) or saline (0.9% NaCl) for another 8 weeks. Food intake and body weight were monitored weekly. Six-week-old male MDX mice were treated with CAY10471 (10 mg/kg, i.p., every other day) or saline (0.9% NaCl) for 6 weeks. Their body weights were measured weekly.

### Metabolic analysis

Mice were singly housed in a Promethion Metabolic Analyzer (Sable Systems, North Las Vegas, NV, USA) at ambient temperature (20–22°C). Prior to the study and data collection, mice were acclimated to calorimetry cages. The O<sub>2</sub> consumption and CO<sub>2</sub> production rates were measured for each mouse for 1 min at 5-min intervals. Energy expenditure was calculated using the Weir equation. Ambulatory activity and position were detected using XYZ beam arrays (BXYZ-R; Sable Systems) with a beam spacing of 1 cm. Data acquisition and instrument control were coordinated using MetaScreen v2.3.15.1, and the raw data obtained were processed using ExpeData Release 1.9.22.

### Glucose tolerance test and insulin tolerance test

For glucose tolerance test (GTT), mice were fasted overnight and injected intraperitoneally with a 20% glucose solution (2.0 g/kg body weight). For insulin tolerance test (ITT), mice were injected intraperitoneally with 1 U/kg after 4 h of fasting. Tail blood samples were collected and measured at 30, 60, 90, 120 and 150 min after injection for analysis using a glucose metre (ACCU-CHEK Performa, Roche).

### Additional methods

Additional details regarding the methods and materials are provided in the supporting information.

### Statistical analysis

Data are expressed as the mean ± standard error of the mean. Data were analysed using GraphPad Prism 8.0 (GraphPad Software). Unpaired two-tailed Student's *t*-test was used for comparisons between two groups. Multiple comparisons were performed using one-way ANOVA with uncorrected Fisher's least significant difference test, two-way ANOVA with the Sidak multiple-comparisons test or repeated measures two-way ANOVA with the Sidak test. A linear mixed model (LMM) was used to analyse the mean mitochondrial length using SPSS software (Version 26.0; IBM Corp., Armonk, NY, USA). Statistical significance was set at  $P < 0.05$ .

## Results

### Deletion of the DP2 receptor increases the proportion of oxidative muscle fibres in mice

PGD<sub>2</sub> signalling is mediated via two G protein-coupled receptors: DP1 and DP2. Interestingly, we found that DP2, rather than DP1, was predominantly expressed in the quadriceps (Quad), tibialis anterior (TA; predominantly glycolytic fibres), gastrocnemius (GC; a mixture of oxidative and glycolytic fibres), extensor digitorum longus (EDL; predominantly glycolytic fibres) and soleus (Sol; predominantly oxidative fibres) muscles of mice (Figure S1A). In mice fed with an HFD, both DP1 and DP2 mRNA expression levels, along with PGD<sub>2</sub> levels, were significantly increased in the EDL and Sol muscles (Figure 1A,B). Strikingly, DP2 KO mice, but not DP1 KO mice, exhibited increased mRNA levels of oxidative fibre markers such as *Myh7* and *Myh2*; reduced mRNA levels of the glycolytic fibre marker *Myh1* in the EDL, Sol and GC muscles (Figure 1C); and higher protein levels of MHC I (encoded by *Myh7*) and MHC IIa (encoded by *Myh2*) in the GC muscles (Figure 1D), when compared with WT mice. Succinate dehydrogenase (SDH) staining confirmed a marked increase in the percentage of oxidative fibres in the TA muscles of DP2 KO mice (Figure 1E). These results indicate that the loss of DP2 promotes glycolytic-to-oxidative muscle fibre transition.

### Skeletal muscle-specific deletion of DP2 enhances exercise tolerance in mice by promoting oxidative muscle fibre transition

To further determine the role of DP2 in skeletal muscles, we generated skeletal muscle-specific DP2 deletion mice by crossing DP2<sup>fl/fl</sup> mice with HSA<sup>Cre</sup> mice. Consistent with the results from the global DP2 KO mice, the loss of DP2 in skel-

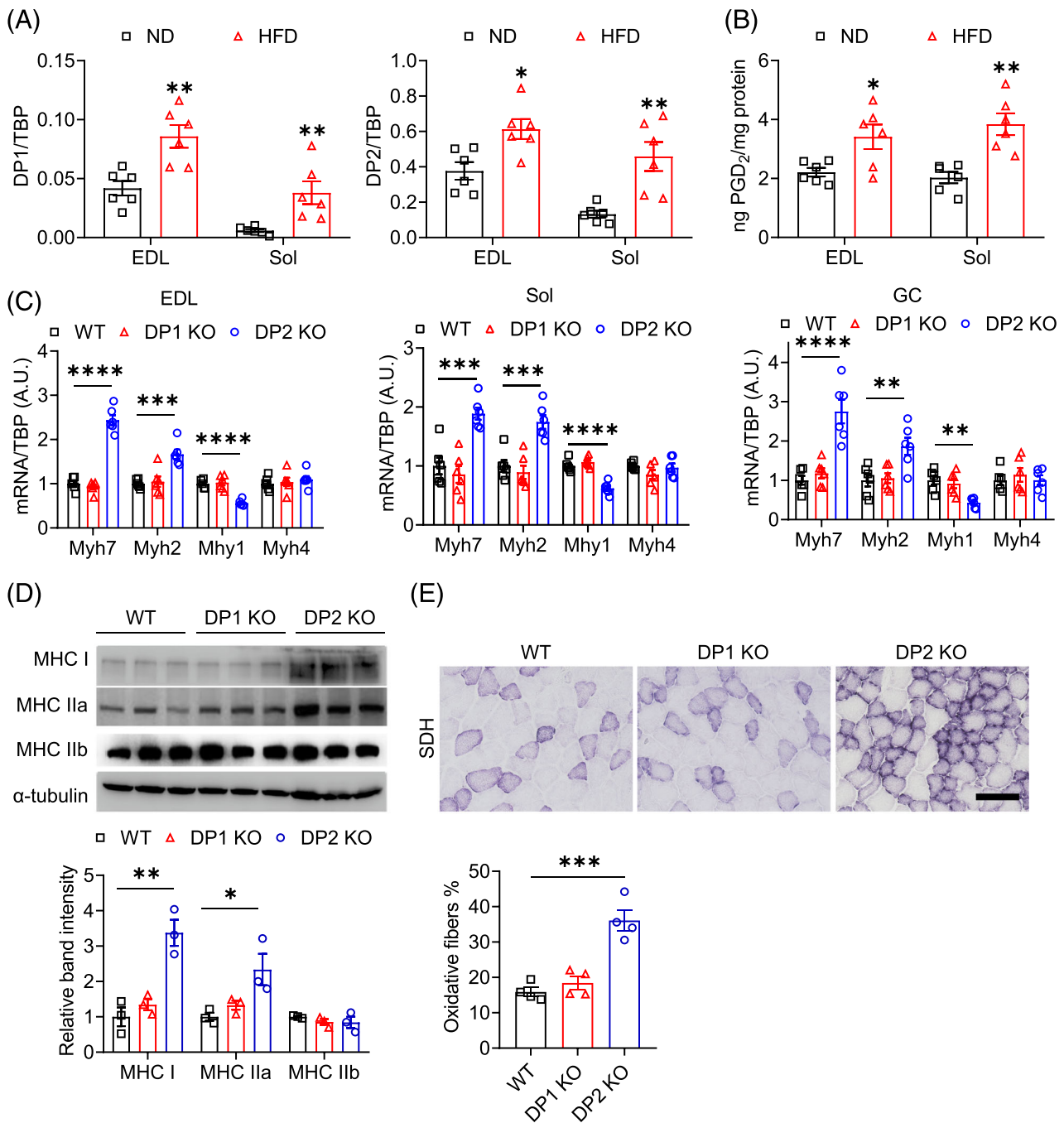


**Figure 1** The ablation of DP2 leads to glycolytic-to-oxidative muscle fibre transition in murine muscles. (A) RT-qPCR analysis of the mRNA levels of *DP1* (left) and *DP2* (right) in the muscles of mice fed a normal chow diet (ND) or a high-fat diet (HFD) for 12 weeks ( $n = 6$ ). (B) Prostaglandin D<sub>2</sub> (PGD<sub>2</sub>) levels in the muscles of mice fed an ND or HFD for 12 weeks ( $n = 6$ ). (C) Relative mRNA levels of type I, IIa, IIx or IIb muscle markers [Myh 7, Myh2, Myh1 and Myh4] in the extensor digitorum longus (EDL) (left), soleus (Sol) (middle) and gastrocnemius (GC) (right) muscles of wild-type (WT), DP1 KO and DP2 KO mice ( $n = 6$ ). (D) Representative image (top) and quantification (bottom) of western blot of myosin heavy chain (MHC) I, IIa and IIb expression in the GC muscles of WT, DP1 KO and DP2 KO mice ( $n = 3$ ). (E) Representative image (top) and quantification (bottom) of the succinate dehydrogenase (SDH) staining of the tibialis anterior (TA) muscles of WT, DP1 KO and DP2 KO mice ( $n = 4$ ). Scale bar, 100  $\mu$ m. Data are expressed as the mean  $\pm$  standard error of the mean (SEM). Statistical significance was determined using an unpaired two-tailed Student's *t*-test. \* $P < 0.05$ , \*\* $P < 0.01$ , \*\*\* $P < 0.001$ , \*\*\*\* $P < 0.0001$  versus ND or WT. AU, arbitrary unit

etal muscles (Figure 2A) also led to a remarkable glycolytic-to-oxidative fibre-type switch in the EDL, Sol, GC and TA muscles of mice (Figure 2B–D). When subjected to a low-intensity run-to-exhaustion exercise protocol on a motorized treadmill, DP2<sup>fl/fl</sup>HSA<sup>Cre</sup> mice showed a significant increase in running duration and distance, with a lower blood lactate concentration (Figure 2E,F). Transmission electron microscopy (TEM) analysis showed that the skeletal muscle mitochondria in DP2<sup>fl/fl</sup>HSA<sup>Cre</sup> mice appeared larger than those in their littermate controls (Figure 3A). Consistently, we also observed a marked increase in the mRNA expression of electron trans-

port chain genes (CI–CIV) and ATP synthase in the Sol muscles of DP2<sup>fl/fl</sup>HSA<sup>Cre</sup> mice (Figure 3B), accompanied by a higher citrate synthase activity (Figure 3C) and mtDNA/nDNA ratio (Figure 3D). Furthermore, primary myoblasts from the hind-limb muscles of DP2 KO mice had higher basal and maximal oxygen consumption rates than in control mice (Figure 3E). Additionally, ATP content was also significantly higher in the Sol and EDL muscles from DP2 KO mice compared with WT mice (Figure 3F). These results indicate that DP2 deficiency in skeletal muscle enhances muscle function by facilitating oxidative muscle fibre transition.

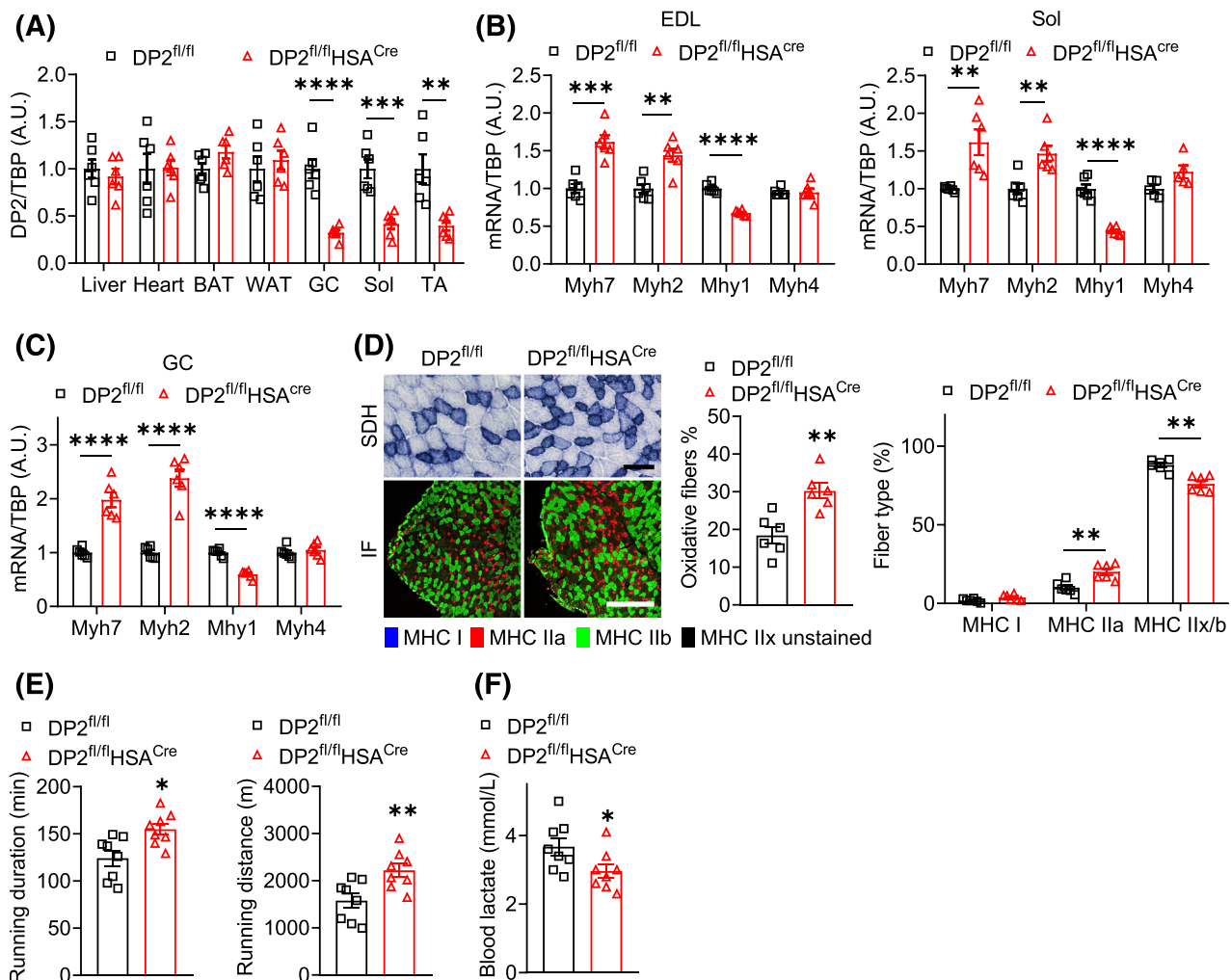


**Figure 2** Skeletal muscle-specific deletion of DP2 enhances endurance exercise performance in mice. (A) RT-qPCR analysis of the mRNA levels of DP2 in various tissues of DP2<sup>fl/fl</sup> and DP2<sup>fl/fl</sup>HSA<sup>Cre</sup> mice. BAT, brown adipose tissue; WAT, white adipose tissue ( $n = 6$ ). (B, C) Relative mRNA levels of myosin heavy chain (*Myh*) 7, *Myh2*, *Myh1* or *Myh4* in the extensor digitorum longus (EDL) (B left), soleus (Sol) (B right) and gastrocnemius (GC) (C) muscles of DP2<sup>fl/fl</sup> and DP2<sup>fl/fl</sup>HSA<sup>Cre</sup> mice ( $n = 5-6$ ). (D) Representative image of succinate dehydrogenase (SDH) and immunofluorescence (IF) staining (left) and quantification (middle for SDH, right for IF) of different fibre markers in the tibialis anterior (TA) muscles of DP2<sup>fl/fl</sup> and DP2<sup>fl/fl</sup>HSA<sup>Cre</sup> mice ( $n = 6$ ). Scale bar: 100  $\mu$ m (SDH), 500  $\mu$ m (IF). (E) Running duration (left) and distance (right) of DP2<sup>fl/fl</sup> and DP2<sup>fl/fl</sup>HSA<sup>Cre</sup> mice subjected to exhaustion exercise on a motorized treadmill ( $n = 8$ ). (F) Blood lactate levels in mice after exhaustive exercise ( $n = 8$ ). Data are expressed as the mean  $\pm$  SEM. Statistical significance was determined using an unpaired two-tailed Student's *t*-test (A–F). \* $P < 0.05$ , \*\* $P < 0.01$ , \*\*\* $P < 0.001$ , \*\*\*\* $P < 0.0001$  versus DP2<sup>fl/fl</sup>. AU, arbitrary unit

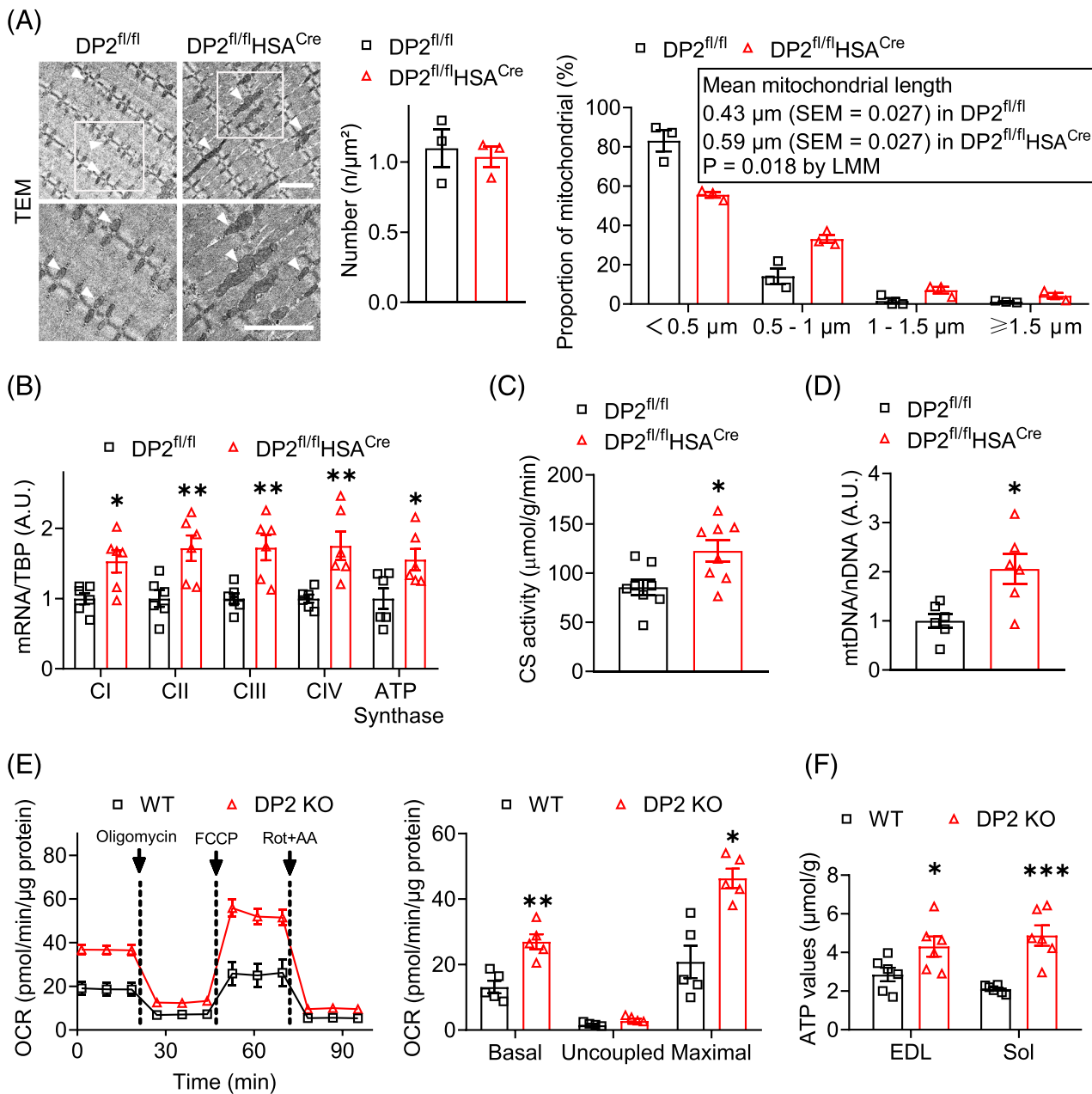


**Figure 3** DP2-deficient skeletal muscles exhibit enhanced oxidative metabolism. (A) Representative transmission electron microscopy (TEM) image (left) and quantification of the number (middle) and length distribution (right) of mitochondria in the soleus (Sol) muscles of DP2<sup>fl/fl</sup> and DP2<sup>fl/fl</sup>HSA<sup>Cre</sup> mice. Arrows indicate the mitochondria ( $n = 3$ ). Scale bar, 2  $\mu\text{m}$ . LMM, linear mixed model.  $P < 0.05$ . (B) RT-qPCR analysis of the mRNA levels of the electron transport chain genes (CI, *Nd1*; CII, *Sdha*; CIII, *Cyc1*; CIV, *Cox7a1*) and ATP synthase in the mouse Sol muscles ( $n = 6$ ). (C) Citrate synthase (CS) activity in the mouse Sol muscles ( $n = 8$ ). (D) Mitochondrial DNA (mtDNA)/nuclear DNA (nDNA) ratio in the mouse Sol muscles ( $n = 6$ ). (E) Oxygen consumption rate (OCR) of primary myoblasts isolated from the mouse hindlimbs. Determination of the OCRs of basal, uncoupled (or proton leak, with oligomycin), maximal (with FCCP) and non-mitochondrial respiration (with rotenone plus antimycin A [Rot + AA]) ( $n = 5$ ). (F) Determination of ATP content in mouse Sol and extensor digitorum longus (EDL) muscle tissues ( $n = 6$ ). Data are expressed as the mean  $\pm$  SEM. Statistical significance was determined using an unpaired two-tailed Student's *t*-test. \* $P < 0.05$ , \*\* $P < 0.01$ , \*\*\* $P < 0.001$  versus DP2<sup>fl/fl</sup> or wild-type (WT). AU, arbitrary unit

### DP2 deficiency in skeletal muscle alleviates high-fat diet-induced obesity and insulin resistance in mice

Skeletal fibre components play an important role in whole-body glucose utilization. Muscle-specific deletion of

DP2 had no obvious effect on body weight, body composition, glucose tolerance or insulin tolerance in mice fed a normal chow diet (Figure S2A–D). When challenged with HFD, DP2<sup>fl/fl</sup>HSA<sup>Cre</sup> mice had lower body weight (Figure 4A), body fat composition (Figure 4B) and serum insulin levels (Figure

4C) and improved glucose tolerance as determined by the GTT and ITT (Figure 4D) compared with their littermate controls. Glycogen content was markedly increased in the skeletal muscles of DP2<sup>fl/fl</sup>HSA<sup>Cre</sup> mice (Figure S3A), whereas there were no significant differences in triglyceride (TG) content in the muscles of DP2<sup>fl/fl</sup>HSA<sup>Cre</sup> and DP2<sup>fl/fl</sup> mice (Figure S3B). In addition, liver lipid accumulation was significantly reduced in DP2<sup>fl/fl</sup>HSA<sup>Cre</sup> mice as determined via haematoxylin and eosin (H&E) and Oil Red O staining (Figure S3C, D). However, the glycogen content in the livers of DP2<sup>fl/fl</sup>HSA<sup>Cre</sup> mice was comparable with that in DP2<sup>fl/fl</sup> mice (Figure S3E). Meanwhile, we observed unchanged food intake (Figure 4E) and locomotor activity (Figure 4F) but a dramatic

increase in total body energy expenditure (Figure 4F) in DP2<sup>fl/fl</sup>HSA<sup>Cre</sup> mice. Thus, the deletion of DP2 in skeletal muscle improves HFD-induced obesity and insulin resistance by accelerating whole-body energy expenditure.

### Deletion of DP2 reprograms myofibers to the oxidative phenotype via RhoA/Rho-associated kinase 2 signalling

As a G protein-coupled receptor, the activation of DP2 dissociates trimeric G proteins into the G<sub>i</sub> and G<sub>βγ</sub> subunits, which in turn triggers complex signalling cascades, such as

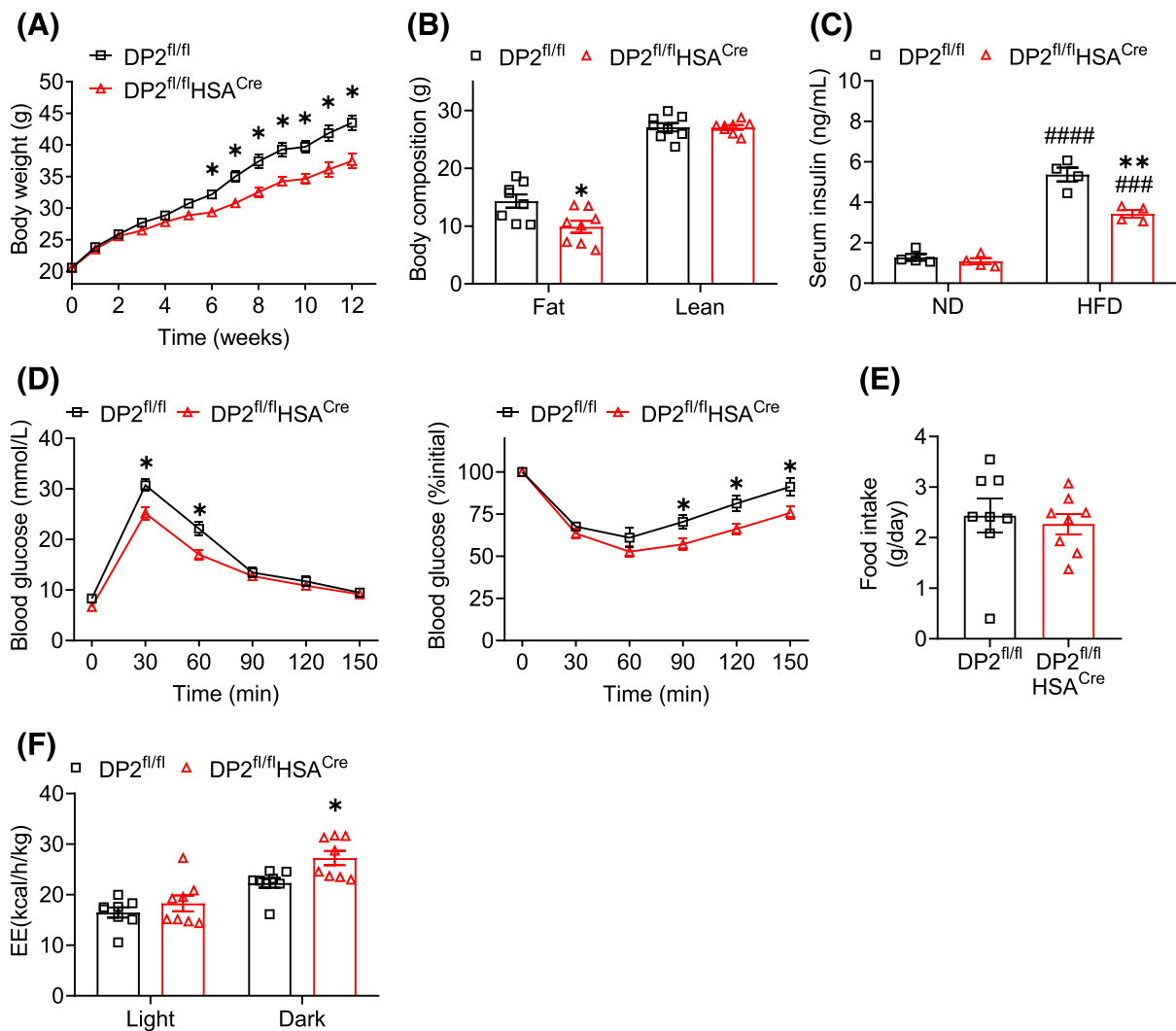


**Figure 4** Skeletal muscle-specific deletion of DP2 improves diet-induced obesity and insulin resistance in mice. (A) Body weights of DP2<sup>fl/fl</sup> and DP2<sup>fl/fl</sup>HSA<sup>Cre</sup> mice fed a high-fat diet (HFD) for 12 weeks ( $n = 8$ ). (B) Lean and fat mass composition of HFD-challenged mice ( $n = 8$ ). (C) Serum insulin levels in HFD-challenged mice ( $n = 4$ ). (D) Glucose tolerance test (GTT) (left) and insulin tolerance test (ITT) (right) in HFD-challenged mice ( $n = 8$ ). (E) Food consumption of HFD-challenged mice ( $n = 8$ ). (F) Average energy expenditure (EE) per hour in HFD-challenged mice during 12/12-h light/dark cycle ( $n = 8$ ). Data are expressed as the mean  $\pm$  SEM. Statistical significance was determined using repeated measures two-way ANOVA with the Sidak test for multiple comparisons (A and D), two-way ANOVA with the Sidak test for multiple comparisons (C and F) or unpaired two-tailed Student's *t*-test (B and E). \* $P < 0.05$ , \*\* $P < 0.01$  versus DP2<sup>fl/fl</sup>; #### $P < 0.0001$ , ##### $P < 0.0001$  versus normal chow diet (ND)

cAMP/protein kinase A (PKA) and phospholipase C-mediated signalling, and mobilizes  $\beta$ -arrestin to activate MAP signalling.<sup>19</sup> We then explored the mechanisms underlying DP2-mediated glycolytic-to-oxidative fibre conversion. During the differentiation of the C2C12 myoblast cell line, treatment with the selective DP2 agonist DK-PGD<sub>2</sub> markedly suppressed the expression of the oxidative myofiber marker *Myh7* and increased the expression of the glycolytic fibre marker *Myh4* (Figure 5A). Strikingly, treatment with the Gi inhibitor pertussis toxin (PTX) rescued the reduced *Myh7* mRNA expression (Figure 5B) and MHC I protein levels in differentiated C2C12 myotubes induced by DK-PGD<sub>2</sub> (Figure 5C). Because cAMP/PKA inhibits RhoA activity<sup>20</sup> and the blockage of RhoA/Rock signalling enhances oxidative fibre generation,<sup>21</sup> we reasoned whether PKA/RhoA signalling is involved in DP2-mediated glycolytic-to-oxidative fibre conversion. We found that treatment with PTX abolished the DK-PGD<sub>2</sub>-induced inhibition of cAMP generation (Figure 5D) and completely abrogated the enhanced RhoA activity

evoked by DK-PGD<sub>2</sub> in C2C12 myoblasts (Figure 5E). Pharmacological blockage of RhoA or ROCK or genetic silencing of ROCK2 rescued the impaired *Myh7* (Figures 5F and 5S5A–D) and MHC I expression (Figure 5S5E) in differentiated C2C12 myotubes upon DK-PGD<sub>2</sub> treatment. These results indicate that the deletion of DP2 facilitates glycolytic-to-oxidative muscle fibre conversion by suppressing RhoA/ROCK2 signalling.

### DP2 activation inhibits oxidative muscle fibre conversion by inhibiting the nuclear translocation of nuclear factor of activated T cells 1

Muscle fibre determination involves the sequential induction of fibre-specific transcription factors, such as NFATc1 and PGC-1 $\alpha$ . In particular, NFATc1 activation governs oxidative fibre generation by promoting oxidative gene expression and concomitantly repressing the expression of glycolytic genes.<sup>6</sup>

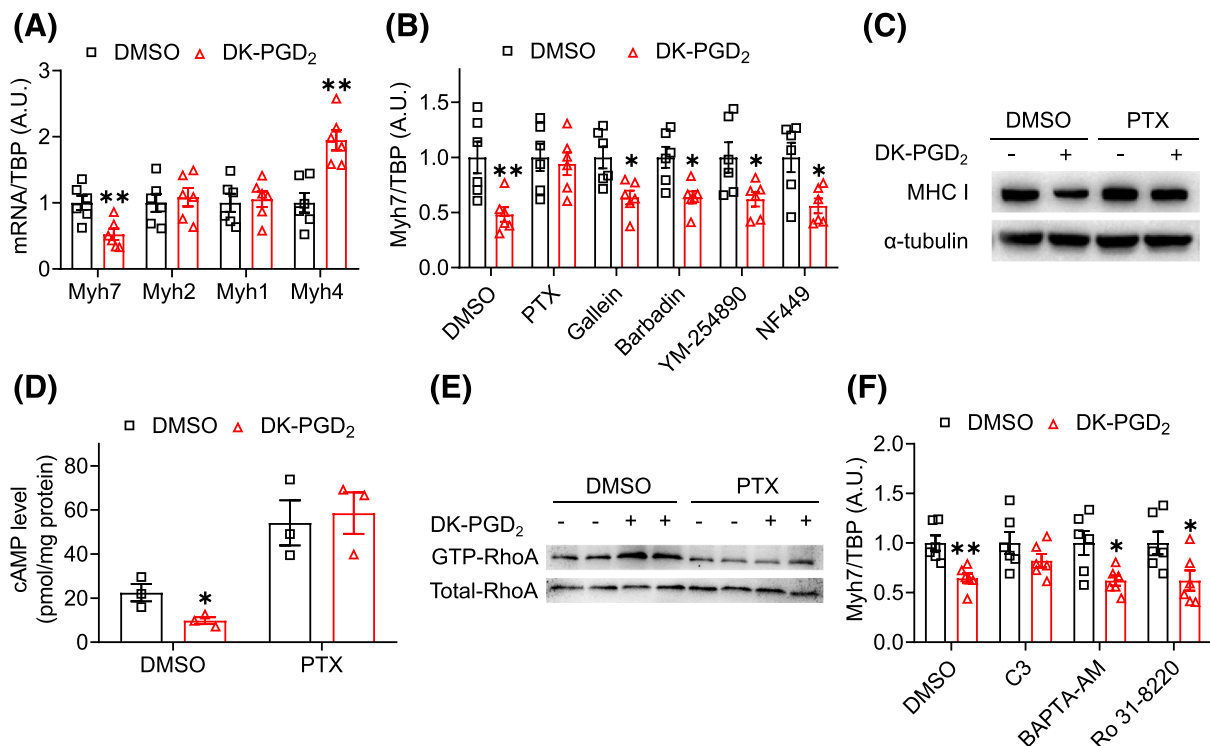


**Figure 5** Activation of DP2 suppresses oxidative muscle fibre switching via RhoA signalling. (A) RT-qPCR analysis of the mRNA levels of myosin heavy chain genes in differentiated C2C12 myotubes after DK-PGD<sub>2</sub> treatment ( $n = 6$ ). (B) Relative mRNA levels of *Myh7* in differentiated C2C12 myotubes treated with the Gi inhibitor, pertussis toxin (PTX) (100 ng/mL); G $\beta\gamma$  inhibitor, gallein (20  $\mu$ M);  $\beta$ -arrestin inhibitor, barbadin (100  $\mu$ M); Gs inhibitor, NF449 (1  $\mu$ M); or Gq inhibitor, YM-254890 (1  $\mu$ M) in the presence or absence of DK-PGD<sub>2</sub> ( $n = 6$ ). (C) Western blot analysis of MHC I expression in differentiated C2C12 myotubes treated with PTX in the presence or absence of DK-PGD<sub>2</sub>. (D) Cellular cAMP levels in C2C12 myoblasts treated with PTX in the presence or absence of DK-PGD<sub>2</sub> ( $n = 3$ ). (E) Western blot analysis of GTP-bound RhoA and total RhoA levels in C2C12 myoblasts treated with PTX in the presence or absence of DK-PGD<sub>2</sub>. (F) Relative mRNA levels of *Myh7* in differentiated C2C12 myotubes treated with the RhoA inhibitor, C3 (1  $\mu$ g/mL); Ca<sup>2+</sup> inhibitor, BAPTA-AM (10  $\mu$ M); or PKC inhibitor, Ro 31-8220 (10  $\mu$ M) in the presence or absence of DK-PGD<sub>2</sub> ( $n = 6$ ). Data are expressed as the mean  $\pm$  SEM. Statistical significance was determined using an unpaired two-tailed Student's *t*-test. \* $P < 0.05$ , \*\* $P < 0.01$  versus dimethyl sulfoxide (DMSO). AU, arbitrary unit

We found that the deletion of DP2 selectively increased the nuclear translocation of NFATc1 in mouse hindlimb muscles and differentiated C2C12 myotubes (Figures S6 and 6A). Pharmacological inhibition of Gi, RhoA or ROCK eliminated the inhibition of nuclear translocation of NFATc1 induced by DK-PGD<sub>2</sub> in differentiated C2C12 myotubes (Figure 6A). It has been shown that ROCK2 inactivates NFATc1 by phosphorylating NFATc1 at Ser243.<sup>21</sup> Transfection of the NFATc1 plasmid mutant at Ser243, but not Ser347, restored the expression of Myh7 inhibited by DK-PGD<sub>2</sub> in differentiated C2C12 myotubes (Figure 6B). Using a phospho-specific antibody, we observed that mutating the Ser243 of NFATc1 to alanine eliminated Ser243 phosphorylation of NFATc1 (Figure 6C). Moreover, the inhibition of Gi, RhoA or ROCK activity abolished the DK-PGD<sub>2</sub>-induced NFATc1 Ser243 phosphorylation in differentiated C2C12 myotubes (Figure 6D). Taken together, the activation of DP2 prevents the translocation of NFATc1 from the cytoplasm to the nucleus by promoting the RhoA/ROCK2 signalling-mediated phosphorylation of NFATc1 at Ser243, thereby suppressing glycolytic-to-oxidative fibre transition (Figure 6E).

### Pharmacological inhibition of DP2 ameliorates diet-induced obesity and insulin resistance in mice

Given the inhibitory effect of DP2 on oxidative muscle fibre generation, we tested whether treatment with a DP2 antagonist could attenuate metabolic disorders in mice. After 12 weeks of feeding with an HFD, the mice were treated with the DP2 antagonist CAY10471 for another 8 weeks (Figure 7A). We found that treatment with CAY10471 significantly decreased body weight (Figure 7B left), body fat composition (Figure 7B right) and serum insulin levels (Figure 7C) and improved glucose tolerance (Figure 7D) in HFD-fed mice. CAY10471 treatment also markedly increased glycogen levels in the skeletal muscles (Figure S7A) without affecting TG levels in the skeletal muscles of HFD-fed mice (Figure S7B). Moreover, it attenuated HFD-induced lipid accumulation in the mouse liver (Figure S7C,D) without affecting glycogen deposition (Figure S7E). Importantly, treatment with CAY10471 had no significant effect on food intake (Figure 7E left) and locomotor activity (Figure S8) but boosted total body energy expenditure

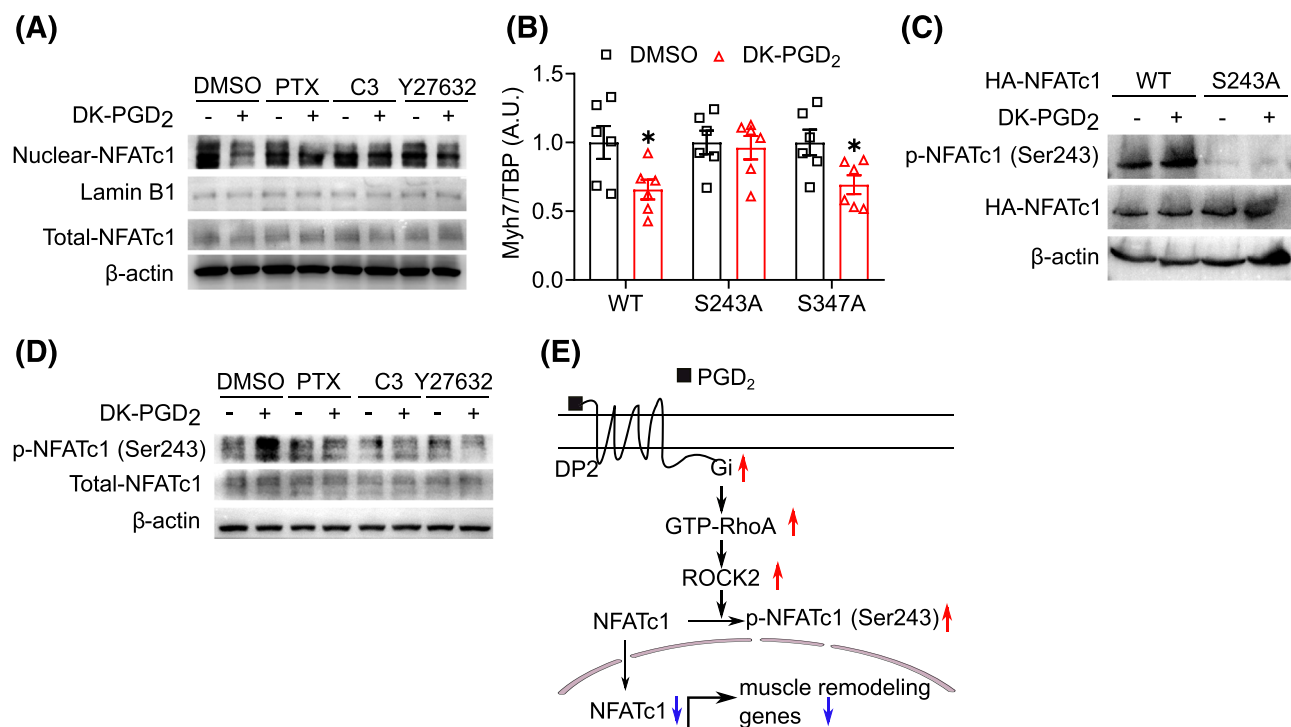


**Figure 6** DP2 activation inhibits nuclear factor of activated T cells 1 (NFATc1)-mediated oxidative muscle fibre transition via the Rho-associated kinase 2 (ROCK2)-mediated phosphorylation of NFATc1 at Ser243. (A) Western blot analysis of the nuclear distribution of NFATc1 in differentiated C2C12 myotubes treated with various inhibitors in the presence or absence of DK-PGD<sub>2</sub>. Gi inhibitor, pertussis toxin (PTX); RhoA inhibitor, C3; ROCK inhibitor, Y-27632. (B) Relative mRNA levels of *Myh7* in differentiated C2C12 myotubes transfected with wild-type (WT) or serine-to-alanine mutant NFATc1 plasmids in the presence or absence of DK-PGD<sub>2</sub> ( $n = 6$ ). (C) Western blot analysis of phosphorylated NFATc1 (p-NFATc1 [Ser243]) levels in differentiated C2C12 myotubes transfected with WT or serine-to-alanine mutant NFATc1 plasmids in the presence or absence of DK-PGD<sub>2</sub>. (D) Western blot analysis of p-NFATc1 (Ser243) and total NFATc1 levels in differentiated C2C12 myotubes treated with PTX, C3 or Y-27632 in the presence or absence of DK-PGD<sub>2</sub>. (E) Schematic illustration of DP2-mediated oxidative myofiber-type conversion via the Gi/RhoA/ROCK2/NFATc1 signalling pathway. Data are expressed as the mean  $\pm$  SEM. Statistical significance was determined using an unpaired two-tailed Student's *t*-test. \* $P < 0.05$  versus dimethyl sulphoxide (DMSO). AU, arbitrary unit

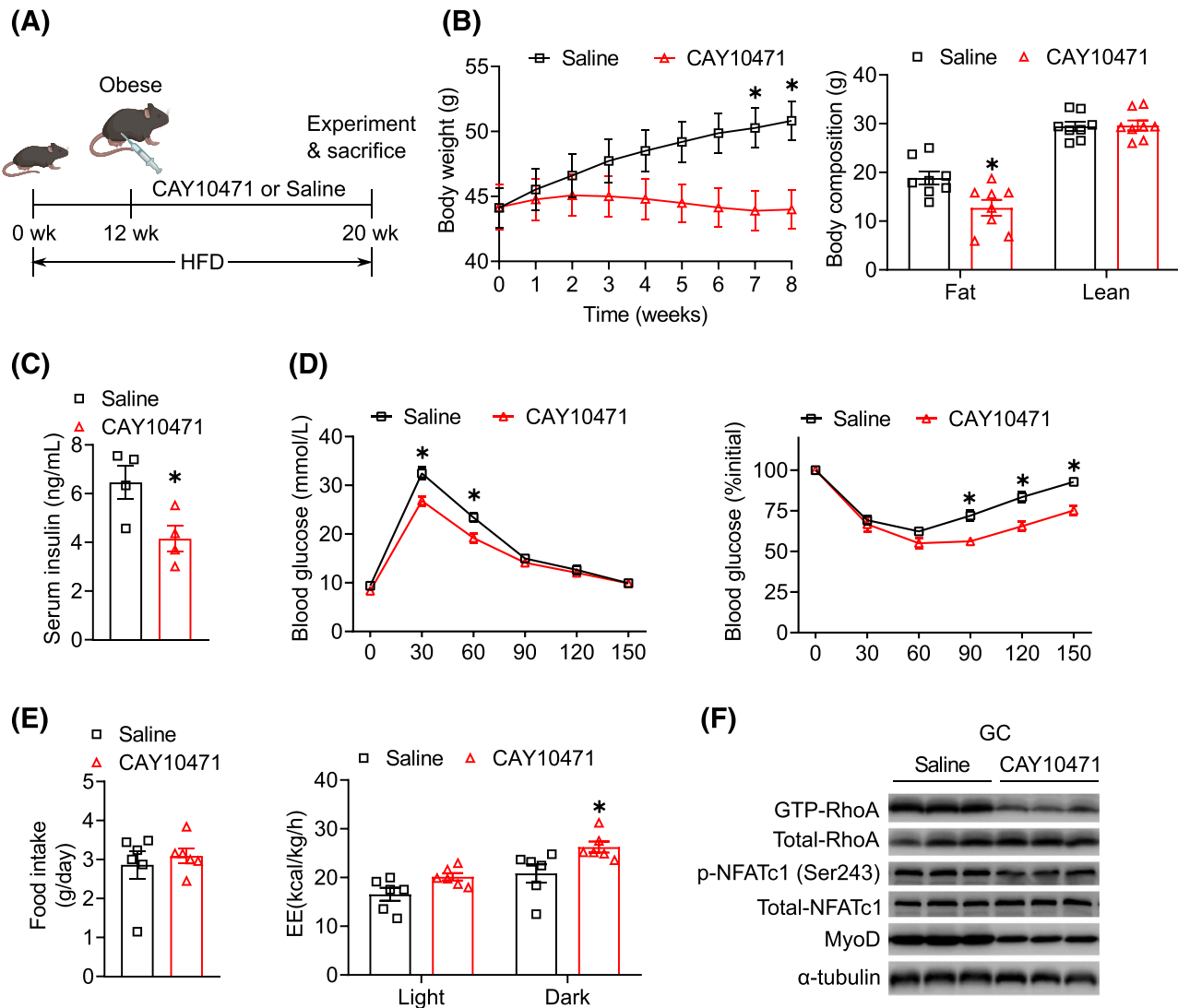


**Figure 7** CAY10471 treatment ameliorates high-fat diet (HFD)-induced obesity in mice. (A) Protocol for the administration of the DP2 inhibitor, CAY10471 (10 mg/kg, i.p., every other day), to mice fed an HFD. wk, week. (B) Body weight (*left*) and body composition (*right*) of mice fed an HFD with or without CAY10471 treatment ( $n = 8$ ). (C) Serum insulin levels in obese mice after CAY10471 treatment ( $n = 4$ ). (D) Glucose tolerance test (GTT) (*left*) and insulin tolerance test (ITT) (*right*) in obese mice after CAY10471 treatment ( $n = 8$ ). (E) Food consumption (*left*) and average energy expenditure (EE) per hour (*right*) in obese mice after CAY10471 treatment ( $n = 6$ ). (F) Western blot analysis of GTP-RhoA, total RhoA, phosphorylated nuclear factor of activated T cells 1 (NFATc1) (p-NFATc1 [Ser243]), total NFATc1 and MyoD protein levels in the gastrocnemius (GC) muscles of obese mice after CAY10471 treatment. Data are expressed as the mean  $\pm$  SEM. Statistical significance was determined using repeated measures two-way ANOVA with the Sidak test for multiple comparisons (B *left* and D), two-way ANOVA with the Sidak test for multiple comparisons (E *right*) or unpaired two-tailed Student's *t*-test (B *right*, C and E *left*). \* $P < 0.05$  versus saline

(Figure 7E *right*) in HFD-fed mice. Finally, CAY10471 treatment significantly suppressed RhoA activity and increased NFATc1 activity, as evidenced by decreased p-NFATc1 (Ser243) levels, which led to reduced MyoD expression (negatively regulated by NFATc1) in the GC muscles of HFD-fed mice (Figure 7F). Thus, DP2 inhibition may alleviate obesity by increasing the proportion of oxidative fibres in mice.

### Pharmacological inhibition of the DP2 receptor improves muscle function in X-linked muscular dystrophy mice

DMD is a lethal, degenerative skeletal muscle disease. The activation of oxidative muscle fibres has been proposed as a therapeutic strategy for DMD.<sup>1</sup> We then investigated

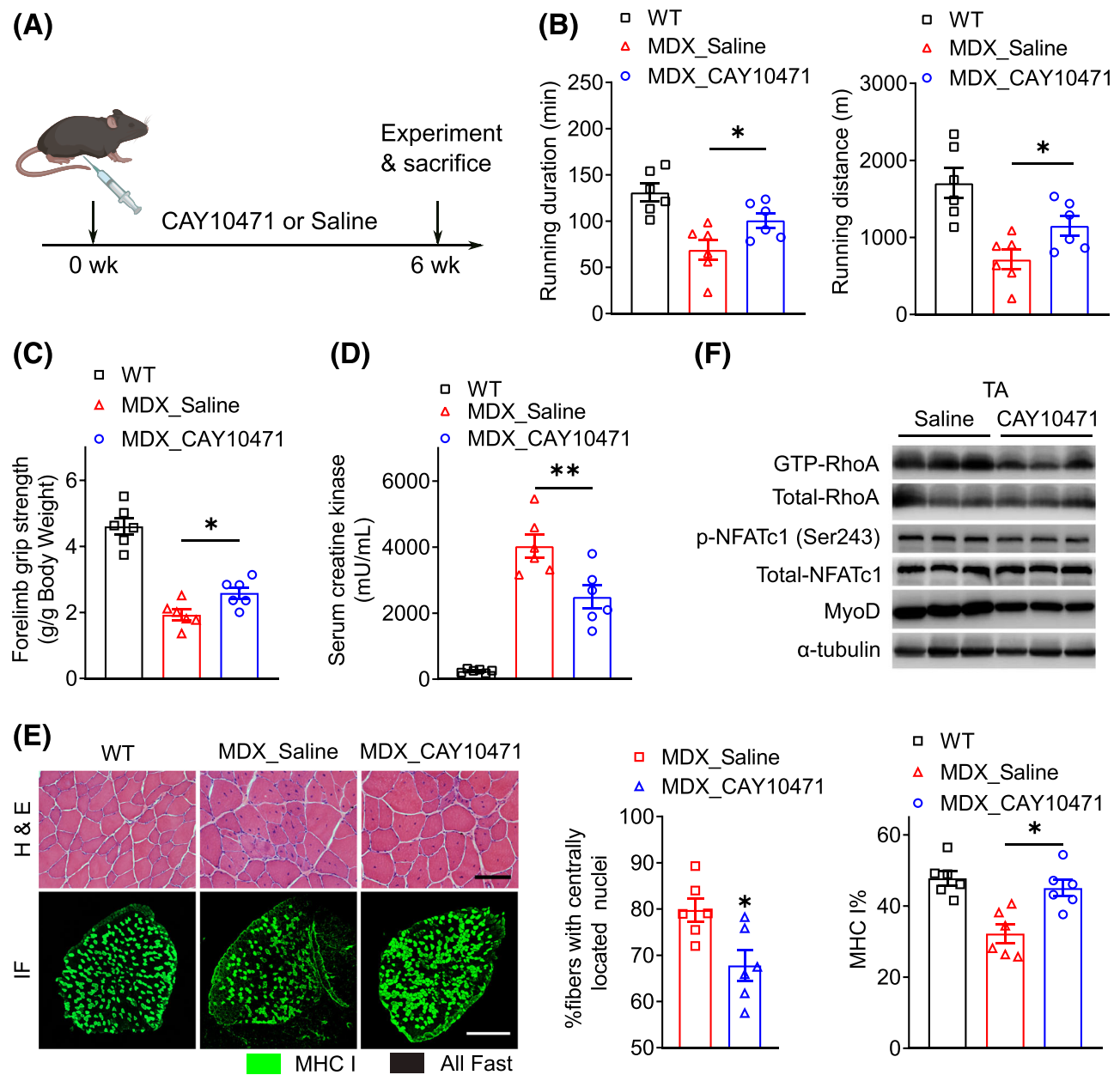


**Figure 8** CAY10471 treatment ameliorates muscle atrophy in X-linked muscular dystrophy (MDX) mice. (A) Protocol for the administration of the DP2 inhibitor, CAY10471 (10 mg/kg, i.p., every other day), to MDX mice. wk, week. (B) Running duration (*left*) and distance (*right*) of CAY10471-treated MDX mice subjected to exhaustive exercise on a treadmill ( $n = 6$ ). (C) Grip strength of CAY10471-treated MDX mice ( $n = 6$ ). (D) Serum creatine kinase (CK) levels in CAY10471-treated MDX mice ( $n = 6$ ). (E) Representative haematoxylin and eosin (H&E)-stained images of the tibialis anterior (TA) and immunofluorescence (IF) staining of the soleus (Sol) muscles (*left*) and quantification of muscle fibres with centrally located nuclei (*middle*) and MHC I muscle fibre percentage (*right*) in CAY10471-treated MDX mice ( $n = 6$ ). Scale bar: 100  $\mu\text{m}$  (H&E), 500  $\mu\text{m}$  (IF). (F) Western blot analysis of GTP-RhoA, total Rho A, MyoD, phosphorylated nuclear factor of activated T cells 1 (NFATc1) (p-NFATc1 [Ser243]) and total NFATc1 protein levels in TA muscles of CAY10471-treated MDX mice. Data are expressed as the mean  $\pm$  SEM. Statistical significance was determined using one-way ANOVA with uncorrected Fisher's least significant difference (LSD) test for multiple comparisons (B–D and E *right*) or unpaired two-tailed Student's *t*-test (E *middle*). \* $P < 0.05$ , \*\* $P < 0.01$  versus MDX\_Saline

whether the inhibition of DP2 could ameliorate DMD by promoting oxidative muscle fibre generation in a mouse model of DMD. We found that both PGD<sub>2</sub> synthesis and DP2 expression were significantly increased in the hindlimb muscles of

MDX mice (Figure S9A,B). Treatment with CAY10471 (Figure 8A) did not significantly affect the body weight (Figure S10), but markedly increased the running duration and distance (Figure 8B) and grip strength (Figure 8C) in MDX mice, as well

as decreased serum creatine kinase levels (Figure 8D). Histological analysis showed fewer regenerated myofibers, as indicated by the decreased number of centrally nucleated fibres and increased number of MHC I fibres (Figure 8E) in the muscles of CAY10471-treated MDX mice. CAY10471 treatment markedly reduced RhoA activity, enhanced NFATc1 activity and suppressed MyoD expression in the hindlimb muscles of MDX mice (Figure 8F). Therefore, the inhibition of DP2 may alleviate DMD by promoting oxidative muscle fibre generation.

## Discussion

PGD<sub>2</sub> plays important roles in skeletal muscle homeostasis and myogenesis; however, the mechanisms underlying these functions are not yet well understood. Here, we identified the PGD<sub>2</sub>/DP2 axis as a critical regulator of skeletal muscle fibre determination. The ablation of DP2 in skeletal muscle cells alleviated diet-induced obesity in mice by promoting the reprogramming of myofibers to the oxidative type by increasing the nuclear translocation of NFATc1. Mechanistically, DP2 activation inhibited oxidative fibre transition by evoking RhoA/ROCK2-mediated NFATc1 phosphorylation at Ser243 and preventing its nuclear translocation. Treatment with a DP2 inhibitor significantly ameliorated diet-induced obesity in mice and improved muscle atrophy in MDX mice.

Accumulating evidence has shown that a smaller proportion of oxidative muscle fibres and a larger percentage of glycolytic fibres (especially type IIx) are associated with a higher body mass index, and patients with obesity have a significantly lower prevalence of oxidative fibres.<sup>22</sup> An increase in relative skeletal muscle mass is inversely associated with incident non-alcoholic fatty liver disease.<sup>23</sup> Notably, PGD<sub>2</sub> levels are significantly increased during obesity and remain high even after weight loss.<sup>24</sup> The deletion of lipocalin-type prostaglandin D synthase (L-PGDS) significantly reduces body weight gain in HFD-fed mice.<sup>25</sup> However, activation of the DP1 receptor suppresses HFD-induced obesity in ApoE<sup>-/-</sup> mice.<sup>26</sup> These results suggested that the DP2 receptor, but not DP1, mediates the pro-obesity effect of PGD<sub>2</sub>. Indeed, we found that PGD<sub>2</sub> levels were also increased in the skeletal muscle tissue, and the genetic ablation of DP2 in skeletal muscle or pharmacological inhibition of DP2 promoted glycolytic-to-oxidative skeletal muscle fibre transition and significantly attenuated HFD-induced obesity and insulin resistance in mice. The blockage of DP2 also inhibited adipogenesis by promoting lipolysis in adipocytes.<sup>27</sup> Hence, DP2 may be a novel therapeutic target for metabolic diseases such as obesity and type 2 diabetes.

DMD is a genetic disorder characterized by progressive muscle loss, chronic inflammation and impaired muscle regeneration. The restoration or activation of oxidative fibre function has been shown to delay and ameliorate the dystrophic phenotype in DMD mouse models.<sup>1,28</sup> During the early onset of

DMD, PGD<sub>2</sub> generation is significantly increased in the skeletal muscles, which in turn aggravates inflammation and causes profound muscle damage.<sup>29</sup> The pharmaceutical inhibition of PGD<sub>2</sub> synthase decreases muscle necrosis and ameliorates dystrophic pathology in patients with DMD.<sup>30</sup> However, the systemic blockage of PGD<sub>2</sub> synthase may also increase the risk of developing hypertension due to the loss of vasodilator and anti-remodelling effects of PGD<sub>2</sub>/DP1 signalling in the vasculature.<sup>31,32</sup> We observed that both DP1 and DP2 were expressed in skeletal muscle cells, but only the disruption of DP2 protected against muscle damage in MDX mice by enhancing glycolytic-to-oxidative fibre transition, suggesting the indispensable role of DP2 in PGD<sub>2</sub>-mediated muscle injury. In addition, DP2 is expressed in Th2 lymphocytes and mediates type 2 inflammation. The depletion of T cells has also been shown to significantly reduce muscle fibrosis in dystrophic mice.<sup>33</sup> Thus, PGD<sub>2</sub>/DP2 axis-mediated Th2 inflammation may also be involved in the pathogenesis of DMD.

The transcription factor NFATc1 acts downstream of Ca<sup>2+</sup>/calcineurin signalling to govern oxidative muscle fibre formation. However, muscular dystrophies are often associated with impaired Ca<sup>2+</sup> homeostasis accompanied by cytosolic Ca<sup>2+</sup> overload and extremely low calcineurin activity.<sup>34,35</sup> The blockage of Ca<sup>2+</sup> channels has almost no clinical benefit in patients with DMD,<sup>36</sup> indicating a compromised Ca<sup>2+</sup>-NFATc1 axis in DMD muscles. Notably, the suppression of RhoA/ROCK2 signalling activates NFATc1 via dephosphorylation of NFATc1 at Ser243 in HFD-challenged skeletal muscles in a Ca<sup>2+</sup>-independent manner.<sup>21</sup> Consistently, we found that DP2 activation markedly increased RhoA/ROCK2 activity, the inhibition of which markedly promoted NFATc1-guided oxidative muscle fibre transformation. Indeed, RhoA/ROCK signalling can impede muscle development at the embryonic stage, and the blockage of ROCK enhances the beneficial effects of corticosteroid treatment in dystrophic mice.<sup>37</sup> PKA activation suppresses RhoA/ROCK signalling in various cell types, including muscle cells, such as cardiomyocytes and smooth muscle cells.<sup>38,39</sup> Similarly, we found that Gi-coupled DP2 inhibited PKA activity to enhance RhoA signalling and suppress NFATc1-mediated oxidative muscle fibre transition. Therefore, the deletion of DP2 attenuates muscular atrophy by facilitating glycolytic-to-oxidative muscle fibre conversion via PKA/RhoA/ROCK/NFATc1 signalling.

In summary, we identified the PGD<sub>2</sub>/DP2 axis as a key regulator for reprogramming myofibers to the oxidative type and that the inhibition of DP2 may represent a novel therapeutic strategy for the treatment of metabolic disorders and DMD.

## Acknowledgements

This work was supported by the National Key R&D Program of China (Grant Number 2021YFC2701104), the National Natural

Science Foundation of China (Grant Numbers 81790623, 82030015, 82225002 and 31771269) and the Key Research Program from Tianjin Municipal Education Commission (Grant Number 2020ZD12). Y. Yu is a fellow at the Jiangsu Collaborative Innovation Center for Cardiovascular Disease Translational Medicine, China. We also thank Anjana Rao (Harvard Medical School and the Center for Blood Research, Boston, MA, USA) for providing the NFATc1 plasmid (Addgene plasmid #11101). All authors of this manuscript certify that they comply with the ethical guidelines for authorship and publication in the *Journal of Cachexia, Sarcopenia and Muscle*.<sup>40</sup>

## Conflict of interest

The authors declare no potential conflicts of interest relevant to this study.

## Online supplementary material

Additional supporting information may be found online in the Supporting Information section at the end of the article.

## References

- Ljubicic V, Burt M, Jasmin BJ. The therapeutic potential of skeletal muscle plasticity in Duchenne muscular dystrophy: phenotypic modifiers as pharmacologic targets. *FASEB J* 2014;**28**:548–568.
- Oberbach A, Bossenz Y, Lehmann S, Niebauer J, Adams V, Paschke R, et al. Altered fiber distribution and fiber-specific glycolytic and oxidative enzyme activity in skeletal muscle of patients with type 2 diabetes. *Diabetes Care* 2006;**29**:895–900.
- Stuart CA, McCurry MP, Marino A, South MA, Howell ME, Layne AS, et al. Slow-twitch fiber proportion in skeletal muscle correlates with insulin responsiveness. *J Clin Endocrinol Metab* 2013;**98**:2027–2036.
- Petchey LK, Risebro CA, Vieira JM, Roberts T, Bryson JB, Greensmith L, et al. Loss of Prox1 in striated muscle causes slow to fast skeletal muscle fiber conversion and dilated cardiomyopathy. *Proc Natl Acad Sci U S A* 2014;**111**:9515–9520.
- Schiaffino S, Reggiani C. Fiber types in mammalian skeletal muscles. *Physiol Rev* 2011;**91**:1447–1531.
- McCullagh KJ, Calabria E, Pallafacchina G, Ciciliot S, Serrano AL, Argentini C, et al. NFAT is a nerve activity sensor in skeletal muscle and controls activity-dependent myosin switching. *Proc Natl Acad Sci U S A* 2004;**101**:10590–10595.
- Bassel-Duby R, Olson EN. Signaling pathways in skeletal muscle remodeling. *Annu Rev Biochem* 2006;**75**:19–37.
- Wang Y, Pessin JE. Mechanisms for fiber-type specificity of skeletal muscle atrophy. *Curr Opin Clin Nutr Metab Care* 2013;**16**:243–250.
- Rovito D, Rerra A-I, Ueberschlag-Pitiot V, Joshi S, Karasu N, Dacleu-Siewe V, et al. Myod1 and GR coordinate myofiber-specific transcriptional enhancers. *Nucleic Acids Res* 2021;**49**:4472–4492.
- Salvatore D, Simonides WS, Dentice M, Zavaacki AM, Larsen PR. Thyroid hormones and skeletal muscle—new insights and potential implications. *Nat Rev Endocrinol* 2014;**10**:206–214.
- Wang T, Xu YQ, Yuan YX, Xu PW, Zhang C, Li F, et al. Succinate induces skeletal muscle fiber remodeling via SUCNR1 signaling. *EMBO Rep* 2019;**20**:e47892.
- Bourdeau Julien I, Sephton CF, Dutchak PA. Metabolic networks influencing skeletal muscle fiber composition. *Front Cell Dev Biol* 2018;**6**:125.
- Korotkova M, Lundberg IE. The skeletal muscle arachidonic acid cascade in health and inflammatory disease. *Nat Rev Rheumatol* 2014;**10**:295–303.
- Velica P, Khanim FL, Bunce CM. Prostaglandin D2 inhibits C2C12 myogenesis. *Mol Cell Endocrinol* 2010;**319**:71–78.
- Mohri I, Aritake K, Taniguchi H, Sato Y, Kamauchi S, Nagata N, et al. Inhibition of prostaglandin D synthase suppresses muscular necrosis. *Am J Pathol* 2009;**174**:1735–1744.
- Kong D, Yu Y. Prostaglandin D2 signaling and cardiovascular homeostasis. *J Mol Cell Cardiol* 2022;**167**:97–105.
- Lin C, Han G, Jia L, Zhao Y, Song J, Ran N, et al. Cardio-respiratory and phenotypic rescue of dystrophin/utrophin-deficient mice by combination therapy. *EMBO Rep* 2022;**23**:e53955.
- Miniou P, Tiziano D, Frugier T, Roblot N, Le Meur M, Melki J. Gene targeting restricted to mouse striated muscle lineage. *Nucleic Acids Res* 1999;**27**:27e–227e.
- Townley RG, Agrawal S. CRTH2 antagonists in the treatment of allergic responses involving TH2 cells, basophils, and eosinophils. *Ann Allergy Asthma Immunol* 2012;**109**:365–374.
- Oishi A, Makita N, Sato J, Iiri T. Regulation of RhoA signaling by the cAMP-dependent phosphorylation of RhoGDI $\alpha$ . *J Biol Chem* 2012;**287**:38705–38715.
- Koo JH, Kim TH, Park S-Y, Joo MS, Han CY, Choi CS, et al.  $\alpha$ 13 ablation reprograms myofibers to oxidative phenotype and enhances whole-body metabolism. *J Clin Invest* 2017;**127**:3845–3860.
- Damer A, El Meniawy S, McPherson R, Wells G, Harper ME, Dent R. Association of muscle fiber type with measures of obesity: a systematic review. *Obes Rev* 2022; e13444.
- Kim G, Lee SE, Lee YB, Jun JE, Ahn J, Bae JC, et al. Relationship between relative skeletal muscle mass and nonalcoholic fatty liver disease: a 7-year longitudinal study. *Hepatology* 2018;**68**:1755–1768.
- Hernandez-Carretero A, Weber N, La Frano MR, Ying W, Lantero Rodriguez J, Sears DD, et al. Obesity-induced changes in lipid mediators persist after weight loss. *Int J Obes (Lond)* 2018;**42**:728–736.
- Fujimori K, Aritake K, Oishi Y, Nagata N, Maehara T, Lazarus M, et al. L-PGDS-produced PGD2 in premature, but not in mature, adipocytes increases obesity and insulin resistance. *Sci Rep* 2019;**9**:1–14, 1931.
- Kumar S, Palaia T, Hall C, Ragolia L. DP1 receptor agonist, BW245C inhibits diet-induced obesity in ApoE<sup>-/-</sup> mice. *Obes Res Clin Pract* 2018;**12**:229–241.
- Wakai E, Aritake K, Urade Y, Fujimori K. Prostaglandin D2 enhances lipid accumulation through suppression of lipolysis via DP2 (CRTH2) receptors in adipocytes. *Biochem Biophys Res Commun* 2017;**490**:393–399.
- Handschin C, Kobayashi YM, Chin S, Seale P, Campbell KP, Spiegelman BM. PGC-1 $\alpha$  regulates the neuromuscular junction program and ameliorates Duchenne muscular dystrophy. *Genes Dev* 2007;**21**:770–783.
- Hoxha M. Duchenne muscular dystrophy: focus on arachidonic acid metabolites. *Biomed Pharmacother* 2019;**110**:796–802.
- Komaki H, Maegaki Y, Matsumura T, Shiraishi K, Awano H, Nakamura A, et al. Early phase 2 trial of TAS-205 in patients with Duchenne muscular dystrophy. *Ann Clin Transl Neurol* 2020;**7**:181–190.
- He Y, Zuo C, Jia D, Bai P, Kong D, Chen D, et al. Loss of DP1 aggravates vascular remodeling in pulmonary arterial hypertension via mTORC1 signaling. *Am J Respir Crit Care Med* 2020;**201**:1263–1276.
- Kong D, Wan Q, Li J, Zuo S, Liu G, Liu Q, et al. DP1 activation reverses age-related hypertension via NEDD4L-mediated T-bet

- degradation in T cells. *Circulation* 2020; **141**:655–666.
33. Farini A, Meregalli M, Belicchi M, Battistelli M, Parolini D, D'Antona G, et al. T and B lymphocyte depletion has a marked effect on the fibrosis of dystrophic skeletal muscles in the scid/mdx mouse. *J Pathol* 2007; **213**:229–238.
34. Duan D, Goemans N, Takeda S'i, Mercuri E, Aartsma-Rus A. Duchenne muscular dystrophy. *Nat Rev Dis Primers* 2021; **7**:1–19, 13.
35. Bella P, Farini A, Banfi S, Parolini D, Tonna N, Meregalli M, et al. Blockade of IGF2R improves muscle regeneration and ameliorates Duchenne muscular dystrophy. *EMBO Mol Med* 2020; **12**:e11019.
36. Phillips MF, Quinlivan R. Calcium antagonists for Duchenne muscular dystrophy. *Cochrane Database Syst Rev* 2008; **4**:CD004571.
37. Rodríguez-Fdez S, Bustelo XR. Rho GTPases in skeletal muscle development and homeostasis. *Cell* 2021; **10**:2984.
38. Sun S, Zhang M, Lin J, Hu J, Zhang R, Li C, et al. Lin28a protects against diabetic cardiomyopathy via the PKA/ROCK2 pathway. *Biochem Biophys Res Commun* 2016; **469**:29–36.
39. Hirakawa M, Karashima Y, Watanabe M, Kimura C, Ito Y, Oike M. Protein kinase A inhibits lysophosphatidic acid-induced migration of airway smooth muscle cells. *J Pharmacol Exp Ther* 2007; **321**:1102–1108.
40. von Haehling S, Morley JE, Coats AJS, Anker SD. Ethical guidelines for publishing in the Journal of Cachexia, Sarcopenia and Muscle: update 2021. *J Cachexia Sarcopenia Muscle* 2021; **12**:2259–2261.